Identification of PRMT5 Inhibitors with Novel Scaffold Structures through Virtual Screening and Biological Evaluations

Lun Zhang
Zhejiang Sci-Tech University
Chenxi Cao
Jiaxing University
Jia Jin
Zhejiang Sci-Tech University
Yaohua Fan
Jiaxing University
Xiaoguang Wang
Jiaxing University
Qian Zhang
Zhejiang Sci-Tech University
Haofeng Hu
Zhejiang Sci-Tech University
Xiaoqing Ye
Zhejiang Sci-Tech University
Lei Wang
Zhejiang Sci-Tech University
Fei Ye (yefei@zstu.edu.cn)
Zhejiang Sci-Tech University https://orcid.org/0000-0003-4119-3219

Research Article

Keywords: PRMT5, small-molecule inhibitors, virtual screening, molecular docking, molecular dynamics simulations

Posted Date: June 17th, 2021

DOI: https://doi.org/10.21203/rs.3.rs-571044/v1

Identification of PRMT5 Inhibitors with Novel Scaffold Structures through Virtual Screening and Biological Evaluations

Lun Zhang[1,#], Chenxi Cao[2,#], Jia Jin[1], Yaohua Fan[2], Xiaoguang Wang[2], Qian Zhang[1], Haofeng Hu[1], Xiaoqing Ye[1,3], Lei Wang[1,*], Fei Ye[1,*]

[1] College of Life Sciences and Medicine, Zhejiang Sci-Tech University, Hangzhou, China

[2] Department of Surgery, The Second Affiliated Hospital of Jia Xing University, Jiaxing, China

[3] Drug Discovery and Design Center, State Key Laboratory of Drug Research, Shanghai Institute of Materta Medica, Chinese Academy of Sciences, Shanghai, China

[#] Lun Zhang and Chenxi Cao contributed equally

[*] Corresponding authors. E-mail addresses: wanglei@ zstu.edu.cn (Lei Wang), yefei@zstu.edu.cn (Fei Ye).

Abstract: Protein arginine methyltransferase 5 (PRMT5), an important member in PRMT family, has been validated as a promising anticancer target. In this study, through the combination of virtual screening and biological experiments, we have identified two PRMT5 inhibitors with novel scaffold structures. Among them, compound Y2431 showed moderate activity with IC_{50} value of 10.09 μM and displayed good selectivity against other methyltransferases. The molecular docking analysis and molecular dynamics (MD) simulations suggested that the compound occupied the substrate-arginine binding site. Furthermore, Y2431 exhibited anti-proliferative activity to leukemia cells by inducing cell cycle arrest. Overall, the hit compound could provide a novel scaffold for further optimization of small-molecule PRMT5 inhibitors.

Keywords: PRMT5, small-molecule inhibitors, virtual screening, molecular docking, molecular dynamics simulations

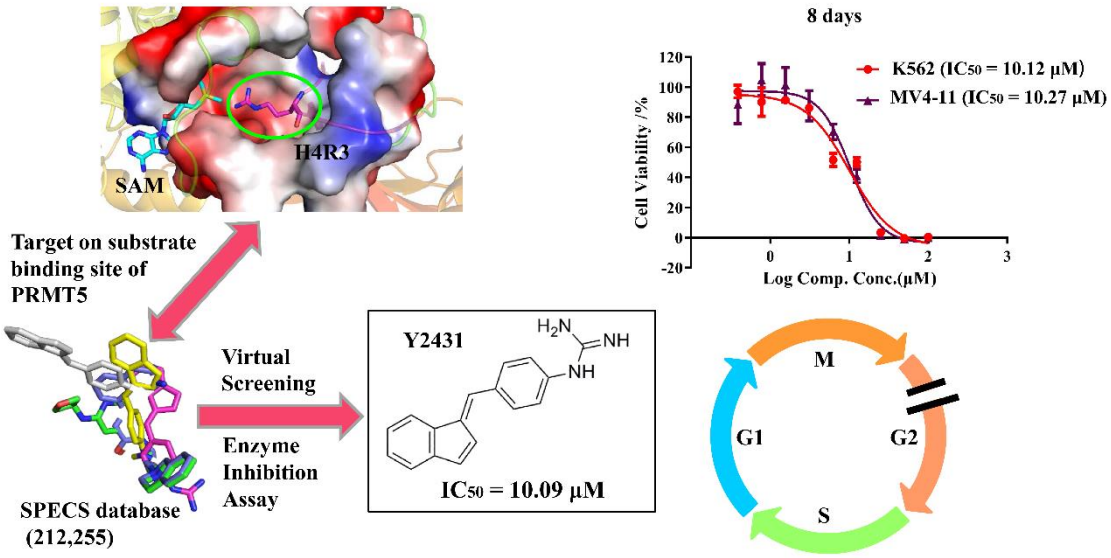

Introduction

Protein arginine methylation is an important posttranslational modification catalyzed by protein arginine methyltransferases (PRMTs). By using S-adenosyl-L-methionine (SAM) as methyl donor, PRMTs catalyze the methylation of arginine residues in a variety of proteins [1]. To date, there are nine members of PRMTs have been reported in mammalian cells. Based on the difference in the catalytic products, they are divided into three forms: Type I (PRMT1, 2, 3, 4, 6, and 8), Type II (PRMT5, 9) and Type III (PRMT7) [2]. Both of type I PRMTS and type II PRMTs could catalyze the formation of monomethylarginines (MMA), type I PRMTs could also catalyze the formation of asymmetric dimethylarginines (ADMA), while type II PRMTs catalyze the production of symmetric dimethylarginines (SDMA). As the only III type PRMTs, PRMT7 solely generates MMA [3].

PRMT5, which is considered to be the main type II PRMT, has a variety of substrates, including histone H2A residue Arg3 (H2AR3), H4 residue Arg3 (H4R3) and H3 residues Arg2 (H3R2) [4]. PRMT5 could regulate transcriptional repression [5], RNA splicing [6], signal transduction [7] and piRNA [8], therefore playing a significant role in diverse cellular processes. Overexpression of PRMT5 is present in many cancers, such as gastric cancer [9], colorectal cancer [10], lymphoma and leukemia [11]. Accordingly, PRMT5 is thought to be an attractive therapeutic target for various cancers.

Due to the important role of PRMT5 in cancer physiology and pathology, it is urgent to develop effective inhibitors. Up to now, great efforts have been made to develop PRMT5 inhibitors (Fig. 1). According to the structure characteristics, they can be classified into SAM analogues (e.g.,

Sinefungin [12], DS-437 [13] and LLY-283 [14]) and non-SAM analogues (e.g., DC_Y134 [15], GSK-3326595 [16], DC-C01 [17] and CMP5 [18]). Among them, GSK-3326595, which exhibits optimal inhibitory activity against PRMT5 at enzymatic level with an IC_{50} of 6.2 nM, has entered into phase Ⅱ clinical trial for the treatment of solid tumors and non-Hodgkin's lymphoma. Considering the value of PRMT5 in tumor therapy, it is significant to search more novel inhibitors with good pharmacological properties targeting PRMT5.

As one of computer aided drug design (CADD) methods, virtual screening has been widely used in academia and industry to discover lead compounds [19]. Previously, we identified compound DC_Y134 as a PRMT5 inhibitor by virtual screening targeting the binding site composed of the SAM-binding pocket and the substrate-binding pocket [15]. Here, to obtain compounds with better selectivity, we fine-tuned our strategies to focus on the arginine-binding pocket, and discovered a new PRMT5 inhibitor which showed good selectivity against other methyltransferases and anti-proliferative activity in several PRMT5-associated cancer cell lines.

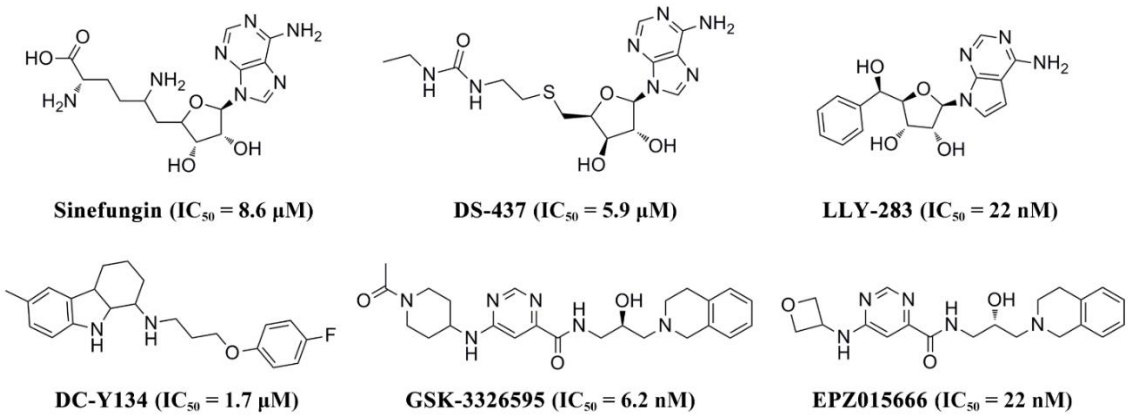

Fig. 1 Reported inhibitors of PRMT5, SAM analogues and non-SAM analogues.

Methods

Protein structure preparation

In this study, the crystal structure of the human PRMT5:MEP50 in complex with substrate H4 peptide was chosen as the receptor (PDB ID: 4GQB) [12]. After deleting the water molecules and partner MEP50 protein, the Protein Preparation Wizard Workflow integrated in the Maestro 9.0 graphical user interface was used to prepare the structure of PRMT5. The pH value was define as 7.0 ± 2.0 and residues within 6 Å around substrate arginine in H4 peptide were defined as binding

sites. Other parameters were set as the default.

Ligand database preparation

212,255 small molecule compounds from Specs database was chosen for virtual screening. To select drug candidates that could be better used by organisms, Lipinski's rule of five [20] was applied to filter the database and "pan-assay interference compounds (PAINS)" [21] were removed with Pipeline Pilot, version 7.5 (Accelrys Software Inc., San Diego, CA). The generating 18,0000 compounds were optimized to generate quality 3D structures with the precise chirality adopting the default settings by LigPrep provided in the Schrödinger suite [22] and the protonation state was generated by Epik with a pH of 7.0 ± 2.0.[23].

Virtual screening

The virtual screening workflow is depicted in Fig. 2a. First of all, the generating 18,000 compounds were screened through Glide [24] SP and XP modes, leading to the top-ranked 300 compounds. Then, to ensure the structural diversity of candidates, the remaining compounds were classified to 30 groups by " Clustering Molecules" protocol in Pipeline Pilot, version 7.5. Considering the interaction of molecules with key residues such as Q309, S310, F327, E444 or F580, one or three compounds were selected from each group. Finally, 80 compounds were selected for subsequent biological evaluations.

***In vitro* PRMT5 enzyme inhibition and selectivity evaluation**

In vitro enzyme inhibitory activities and selectivity assay of compounds were tested by Shanghai Chempartner Co., Ltd. using ^{3}H-labeled radioactive methylation and AlphaLISA assay, which were adopted by the same protocol as described previously [17, 25, 26]. The PRMT5 protein was purchased from BPS, (Cat. No. 51045) for enzyme activity inhibition test and adding SAH only is control assays. The following formula (eq 1) [26] was used to calculate the inhibition rate:

$$\%\ \text{inhibition} = (\max\ \text{signal} - \text{compound}\ \text{signal})/(\max\ \text{signal} - \min\ \text{signal}) \times 100 \quad (1)$$

The reaction value of enzyme and substrate is the maximum signal; the reaction value of substrate only is the min signal.

The IC_{50} values were analyzed in GraphPad Prism 8.0 software with eq2 [26] and the compound with lowest IC_{50} was choose for selective evaluating:

$$\%\ \text{inhibition} = \text{bottom} + (\text{top} - \text{bottom})/(1 +$$

$10^{((\mathrm{LogIC_{50}} - \text{compound concentration}) \times \text{Hill slope})}$)(2)

In selectivity assay, five other different types of methyltransferases were chosen for further investigation, including representatives of type I arginine methyltransferase (PRMT1, PRMT4), DNA methyltransferase 1 (DNMT1), enhancer of zeste homolog 2 (EZH2), histone methyltransferase G9a and lysine-specific demethylase 1 (LSD1) and compound concentration is 50 μM and 100 μM. Except for DNMT1 and PRMT5, which was detected by radioactive methylation, all the enzymes were analyzed by AlphaLISA and the eq 1 was carried out to calculate the inhibition value.

Molecular dynamics simulation

Molecular dynamics simulations (MD) was performed using Amber14 software (University of California, San Francisco) [27, 28] package. The small molecules were parametrized using the generalized AMBER force field (GAFF) [29] and AM1-BCC charge model [30] by antechamber [31]. The tleap module was employed to generate the topology of each system. Before MD simulations, all the systems were solvated into the TIP3P [32] water box with a 10 Å buffer distance between the box wall and the nearest solute atoms. Na^+ ions were added to neutralize the simulation systems. The three systems were subsequently minimized with the Amber ff14SB force field. After minimization, each system was heated from 0 to 300K within 100 ps, then 1 ns equilibration was carried out. Finally, 80 ns MD simulations on each system were then carried out using the pmemd.cuda module with constant temperature (NPT), and periodic boundary condition. The CPPTRAJ [33] program was applied for all MD trajectory analyses and the VMD software was used to perform visual observation [34]. In order to facilitate the analysis, the conformation of 8000 frames is converted into 800 frames with 10 frames as an extraction interval.

MM/GBSA calculations

The MM/GBSA method [35] in Amber14 was implemented to calculate binding free energies of PRMT5 complex. From the molecular dynamics trajectory, 100 snapshots of the last 10 ns were carried out on the MD trajectory. The equation (eq 3, (eq 4) of binding free energy (ΔG) is:

$$\Delta G_{bind} = G_{complex} - \left(G_{protein} + G_{ligand}\right) \quad (3)$$

$$\Delta G_{bind} = \Delta E_{mm} + \Delta G_{solv} - T\Delta S \quad (4)$$

Molecular mechanics energy (ΔE_{mm}) is the sum (eq 5): of internal energy contributions ($\Delta E_{internal}$), electrostatic contributions ($\Delta E_{eletrostatic}$) and van der Waals terms (ΔE_{vdw}):

$$\Delta E_{MM} = \Delta E_{internal} + \Delta E_{electrostatic} + \Delta E_{vdw} \quad (5)$$

Desolvation free energy (ΔG_{solv}) is the sum (eq 6): of the polar (ΔG_{pol}) and non-polar (ΔG_{nonpol}) contributions:

$$\Delta G_{solv} = \Delta G_{pol} + \Delta G_{nonpol} \quad (6)$$

TΔS is entropic contribution to ΔG at absolute temperature T

Free energy decomposition of inhibitor-residue pairs

Determining the energy contribution of inhibitor-residue pairs to estimate the components in the interactions between the residue and ligand is important [36]. In the current study, residues within the range of PTMT5 substrate active site 12 Å are selected for calculation, and pairwise decomp with 1-4 terms (1-4 EEL and 1-4 VDW) were added to internal prospective terms.

Anti-proliferative assay

According to the results of enzymatic activity tests, we discovered that Y2431 possesses predominant inhibitory activity against PRMT5 *in vitro*. To further explore whether it would affect the proliferation of human Leukemia cell line, MV4-11 and K562 were adopted to assess the inhibitory effect of Y2431 on cancer cells. The cells survival rate was measured using the WST−1 Cell Proliferation Assay Kit. Two cells were seeded in 96-well plates and adding RPMI 1640 medium with 10% fetal bovine serum and then treated with Y2431 at different concentrations or DMSO control for 8 days in a cell culture incubator at 37°C with a supply of 5% CO_2. WST−1 solution was added according to the user guide. Three repetition and replicates were done in each assay. The data of IC_{50} were obtained by GraphPad Prism 8.0.

Cell-Cycle Assays

K562 cell line was plated in 6-well plates and then cultured with Y2431 at a diverse mix of concentrations or DMSO. After 48h, cells collected were re-suspended in 70% ethanol and fixed overnight at 4°C. After washing with PBS, the cells were incubated with Propidium Iodide/RNaseA at room temperature for 30 minutes and detected using flow cytometer (ACEA NovoCyte).

Results and discussion

Virtual screening against substrate-binding pocket

To date, a number of crystal structures of human PRMT5 have been determined, which indicate

that PRMT5 possess two ligand binding sites of cofactor SAM and substrate arginine. Previously, we identified several PRMT5 inhibitors by virtual screening targeting the pocket that contains the two ligand binding sites [15]. Contrast to the binding site of SAM, the protein sequence of substrate-binding site varies in different PRMTs. Consequently, to obtain more PRMT5 small-molecule inhibitors with good selectivity, an optimized approach that focused on substrate-binding site was carried out. Here, the crystal structure of PRMT5 with H4 peptide (PDB ID: 4GQB) was adopted as the target for the following virtual screening procedures, and the flowchart is shown in Fig. 2a. First, Glide SP and XP modes were employed to dock 180,000 prepared ligands into the defined binding pocket. Subsequently, the top-ranked 300 candidates were clustered into 30 groups, and then one or three compounds were selected from each group. Finally, 80 compounds were purchased for the following biochemical evaluation.

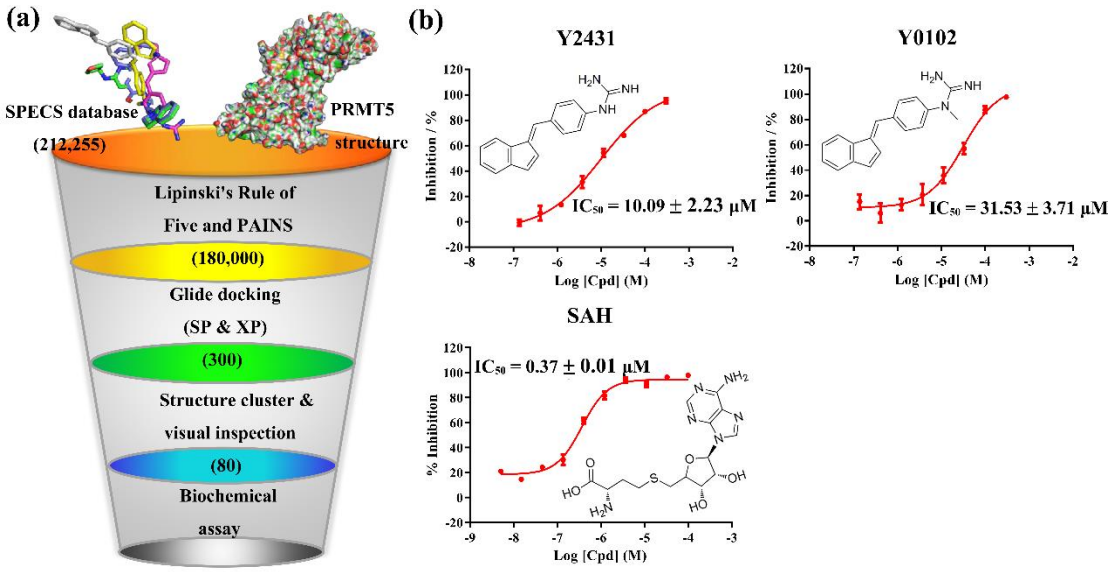

Fig. 2 (a) Schematic representation of the virtual screening procedure. **(b)** The chemical structures and IC_{50} values of compound Y2431, Y0102 and control SAH respectively

Enzyme inhibition and selectivity assay

The 80 compounds selected by virtual screening were tested for PRMT5 inhibitory activity by ^{3}H-labeled radioactive methylation assay. Among these candidates, two compounds (Y2431, Y0102) inhibited PRMT5 activity with IC_{50} values of 10.09 μM and 31.53 μM respectively (Fig. 2b).

Subsequently, we tested the selectivity of the compound Y2431 against other methyltransferases including PRMT1, PRMT4, DNMT1 EZH2, G9a and LSD1. As shown in Table

1, Y2431 exhibited much lower inhibition against other methyltransferase, demonstrating that this compound is a selective inhibitor for PRMT5.

Table 1 *In vitro* inhibitory effects (inhibition rate at 100 μM and 50 μM) of compound Y2131 on the methyltransferase activities of PRMT1, PRMT4, EZH2, LSD1, G9a and DNMT1

Enzyme	% inhibition at 100 μM	% inhibition at 50 μM
PRMT1	17%	13%
PRMT4	11%	10%
EZH2	18%	14%
LSD1	17%	13%
G9a	14%	11%
DNMT1	13%	7%

Molecular dynamics simulation

To investigate the dynamics and energy properties of the two PRMT5/SAM/inhibitor complexes and PRMT5/SAM system, 80 ns molecular dynamics simulations were carried out. The Fig. 3a showed dynamic stability of the three systems during simulations. We monitored root mean square deviation (RMSD) values of protein backbone relative to the initial structure along the entire MD trajectories, which suggested that all of the three systems reached equilibrium states after 70 ns. To investigate the dynamic features, root mean square fluctuation (RMSF) values were also calculated, which revealed the fluctuations of residues are similar in the three systems, especially for the residues near the substrate binding site, indicating that binding of the two inhibitors has little effect on the flexibility of residues in PRMT5 (Fig. 3b). Since the initial structures for MD simulation didn't contain the partner MEP50 protein, the residue fluctuations of the two regions binding to MEP50 (residues 54-74 and 158-180) significantly increased [37]. Radius of gyration (Rg) is a parameter representing the compactness of protein. To estimate the effects of Y2431 and Y0102 bindings on protein, Rg values for the three systems were calculated (Fig. 3c), which showed that the difference between the three protein systems was only 0.5Å after 70ns, indicating that the looseness of the protein does not change much and the conformation is quite stable, which is consistent with the RMSD analysis results.

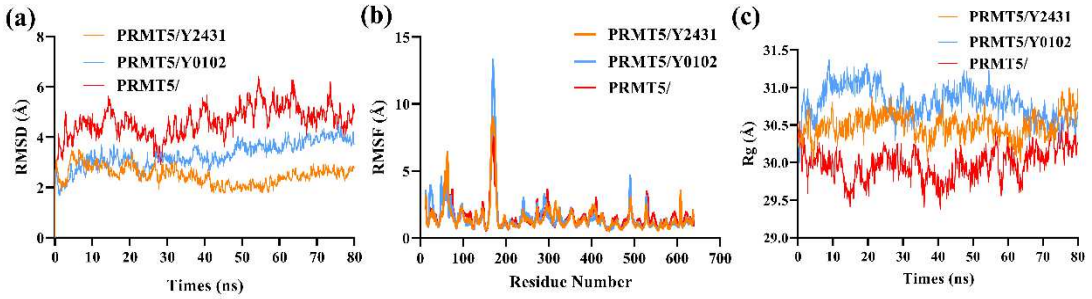

Fig. 3 MD simulations results. RMSD (**a**), RMSF (**b**) and Rg (**c**) analysis over the entire 80 ns MD trajectory of PRMT5 (red) and PRMT5 complexes with compound Y2431 (orange lines) and Y0102 (blue lines), respectively

Binding free energy analysis

Based on the results of MD simulations, MM/GBSA method was utilized to calculate the binding free energy of the two compounds with PRMT5. As shown in Table 2, compound Y2431 binds to PRMT5 with a ΔG value of -25.77 kcal/mol, while Y0102 only got a ΔG value of -16.28 kcal/mol, indicating that Y2431 has a higher binding affinity with PRMT5, which is consistent with the experimental data of bioassays. Besides, the energy component of van der Waals (ΔE_{vdw}) is favorable for the binding of both compounds, while the polar solvation is not beneficial for the binding.

Table 2 Binding free energy and its individual components in kcal/mol calculated by the MM/GBSA method

Inhibitors	ΔE_{ele}	ΔE_{vdw}	ΔG_{nonpol}	ΔG_{pol}	ΔG_{bind}
Y2431	-207.57	-31.19	-4.51	217.49	-25.77
Y0102	-180.88	-25.42	-3.48	193.50	-16.28

To obtain a detailed view of the protein-inhibitor binding, the binding energy of the residues in the substrate binding pocket was decomposed to investigate the partial energy contributions of each residue upon substrate binding. The residues that have a contribution of < -1 kcal/mol were summarized in Table 3, suggesting that some residues that play important roles in substrate H4 peptide binding [12] are also critical for inhibitors binding, especially for Y2431.

Subsequently, we compared the energy contribution components of the key residues that are important for binding of H4 peptide [12]. As shown in Fig. 4a, compared to Y0102, most of the key residues formed stronger van der Waals interactions with Y2431, except for the residues Y304 and L312. Meanwhile, the electrostatic interactions between these key residues and Y2431 are also stronger, especially for the residue E435 and E444 that form the catalytic active site of PRMT5 (Fig. 4b), providing a molecular basis to explain the inhibitory activity of Y2431 towards PRMT5.

Table 3 Total energy decomposition of inhibitor-residue pairs for active residues

Residues	PRMT5/Y2431 (kcal/mol)	Residues	PRMT5/Y0102 (kcal/mol)
Q322	-4.32	F300	-3.66
T323	-3.61	Y304	-3.59
Q309	-3.47	T323	-2.54
F327	-3.34	F327	2.46
S578	-3.26	V326	-1.81
F580	-2.43	K302	-1.67
W579	-2.17	L299	-1.61
E320	-1.80	F580	-1.10
Q313	-1.40		
Y304	-1.26		
Y307	-1.01		

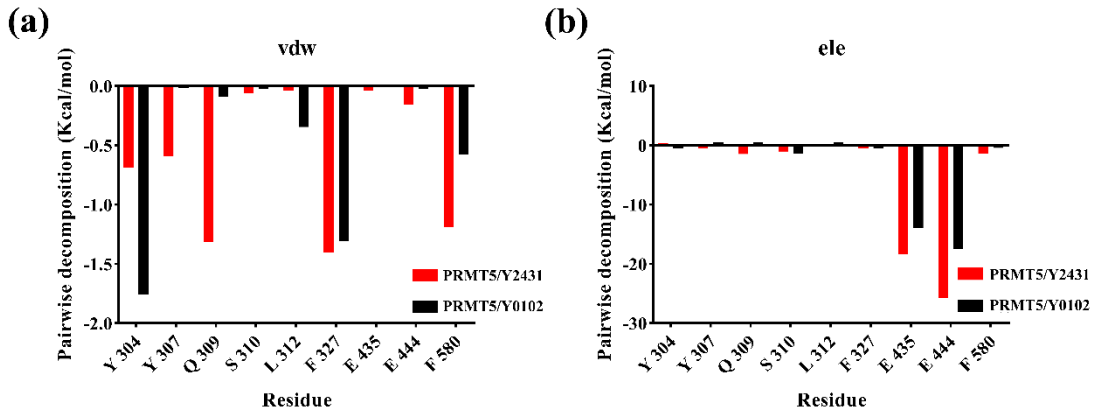

Fig. 4 The energy decomposition of active site amino acids into components. The contribution of vdw (**a**) and electrostatic (**b**) interactions, respectively

Binding mode analysis of PRMT5/Y2431 complex

In order to disclose the binding modes of Y2431 with PRMT5, we extracted the structure of last frame (80 ns) from the MD trajectory to analyze molecular interaction pattern. As shown in Fig.5a, Y2431 occupies the binging site of residue Arg3 in the substrate H4 peptide, while the methyl group of Y0102 almost deviates from the arginine pocket, providing further proof for the results of biochemical experiments. Furthermore, Y2431 fits into the hydrophobic pocket which is made up of residues W579, F580, T323, Q309, V307, V326, Q322, S578 (Fig. 5b-c). In particular, hydrogen bond is formed between the nitrogen in guanidine group and the carbonyl oxygen of residue S578. In addition, E435 and E444 also form electrostatic interactions with the guanidine group of Y2431. Overall, these docking results could reasonably explain the inhibitory activities of Y2431 on PRMT5 *in vitro*.

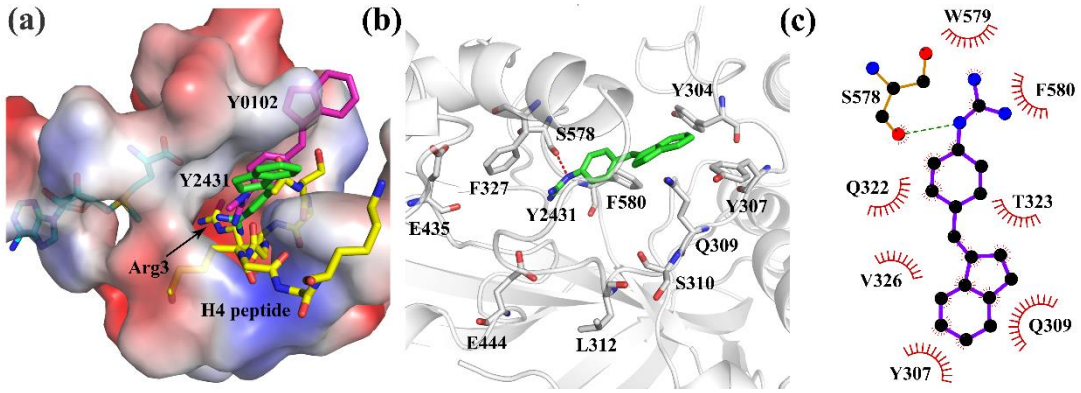

Fig. 5 Putative binding mode of Y2431. **(a)** Superimposition of compound Y2431, Y0102 and H4 peptide (PDB ID 4GQB). Y2431, Y0102 and H4 peptide are shown as green, magenta and yellow sticks respectively, and PRMT5 is depicted in vacuum electrostatic surface. **(b)** Binding mode of Y2431, which is shown as green sticks, and key residues are shown as gray sticks. Hydrogen bonds are shown as red dashed lines. **(c)** Diagrammatic sketch showing putative interactions between PRMT5 and Y2431. Residues involved in the hydrophobic interactions are shown as starbursts, and hydrogen bonds are denoted by dotted green lines

Anticancer Activity and cycle arrest analysis

Since PRMT5 is a potential target of leukemia, two human Leukemia cell lines, MV4-11 and K562 were adopted to test the inhibitory effect of Y2431 on cancer cells. As shown in Fig. 6a-b,

Y2431 could inhibit the proliferation of MV4-11 and K562 cells with IC_{50} values of 10.27 μM and 10.12 μM at 8 days respectively, suggesting a very good cell membrane permeability of this compound. To further investigate the anti-proliferation mechanism of Y2431 towards K562 cells, flow cytometric was carried out to assess the effect on cell cycle. The Fig. 6c indicated that Y2431 arrested the cell cycle in the G2/M phase in a concentration-dependent manner upon treatment for 48h, which revealed the cytotoxic activity of Y2431 against PRMT5-releated leukemia cells.

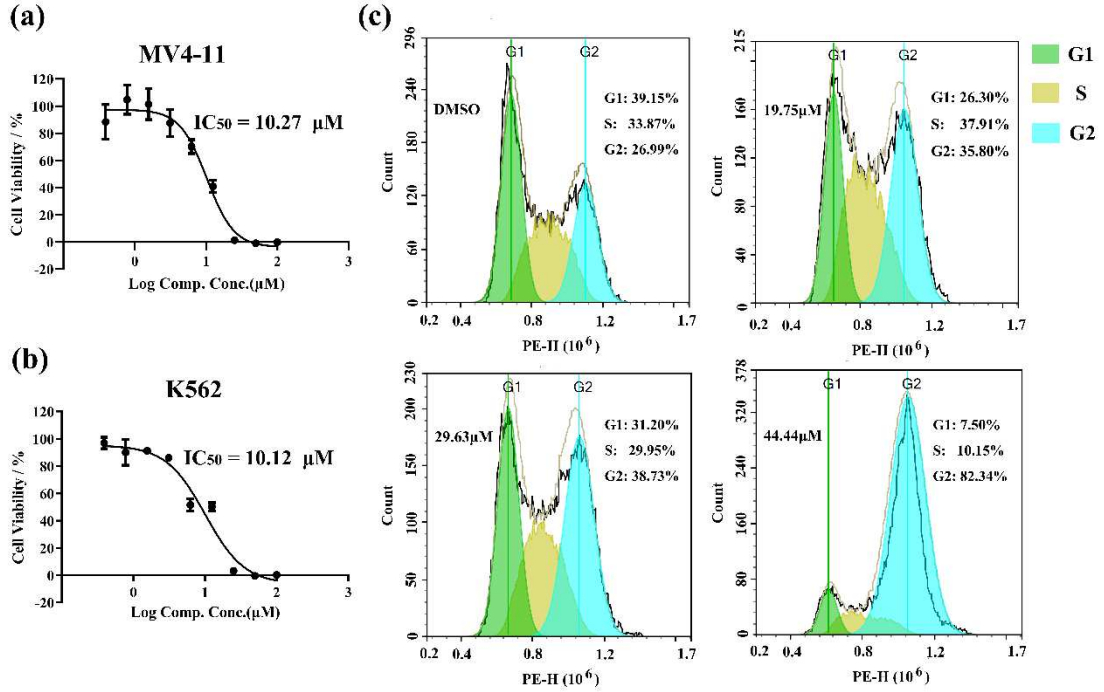

Fig. 6 Cells proliferation inhibition and cycle arrest analysis. **a-b** Antiproliferative effect of Y2431 on MV-411 and K562 cell lines for 8 days. **c** Cell cycle of K562 cell was arrested at G2 phase after treatment with Y2431 for 48h

Conclusion

In conclusion, as one of the most promising biological anticancer targets in the PRMT family, PRMT5 has attracted more and more attention. In this study, through virtual screening and biological evaluations, compound Y2431 has been discovered as a novel PRMT5 inhibitor with IC_{50} values of 10.09 μM. Notably, Y2431 displayed good selectivity against other methyltransferases. Furthermore, MD simulations and binding free energy analysis revealed that Y2431 has a stronger binding affinity with PRMT5 than compound Y0102, which was consistent with inhibitory data. The binding free energy decompositions and binding mode analysis suggested that Y2431 occupied the substrate-

binding pocket. Notably, the electrostatic interactions between positively charged guanidine group and the charged negatively binding pocket play a significant role in the binding of Y2431. E444, which is one of methyltransferase catalytic residues, interacts with Y2431 through electrostatic attraction. These results provided a molecular basis for explaining the inhibitory activity of Y2431 toward PRMT5. In addition, Y2431 also has good cell membrane permeability and can inhibit the proliferation of several PRMT5-related cancer cells. In summary, this study provided a reliable structure-based virtual screening method for identifying novel PRMT5 inhibitors, as well as a novel chemical scaffold for further optimization.

Declarations

Funding: This study was supported by National Natural Science Foundation of China (81803339 to J.J.) and Jiaxing Science and Technology Project (2018AY32002 to C.C.).

Conflicts of interest: The authors declare no competing interest.

Availability of data and material: The datasets used or analyzed during the current study are available from the corresponding author on reasonable request.

Authors' contributions: All authors contributed to the study conception and design. Project design, manuscript editing were performed by Fei Ye, Lei Wang and Jia Jin. Material preparation, data collections, and results analysis were performed by Lun Zhang, Chenxi Cao, Yaohua Fan, Xiaoguang Wang, Qian Zhang, Haofeng Hu and Xiaoqing Ye.

References

[1] Bedford, M.T., Clarke, S.G. Protein arginine methylation in mammals: who, what, and why. Molecular cell. 2009, 33, 1-13.

[2] Di Lorenzo, A., Bedford, M.T. Histone arginine methylation. FEBS letters. 2011, 585, 2024-31.

[3] Feng, Y., Maity, R., Whitelegge, J.P., Hadjikyriacou, A., Li, Z., Zurita-Lopez, C., et al. Mammalian protein arginine methyltransferase 7 (PRMT7) specifically targets RXR sites in lysine- and arginine-rich regions. The Journal of biological chemistry. 2013, 288, 37010-25.

[4] Hu, H., Qian, K., Ho, M.C., Zheng, Y.G. Small Molecule Inhibitors of Protein Arginine Methyltransferases. Expert opinion on investigational drugs. 2016, 25, 335-58.

[5] Pal, S., Vishwanath, S.N., Erdjument-Bromage, H., Tempst, P., Sif, S. Human SWI/SNF-Associated PRMT5 Methylates Histone H3 Arginine 8 and Negatively Regulates Expression of ST7 and NM23 Tumor Suppressor Genes. Molecular and Cellular Biology. 2004, 24, 9630-45.

[6] Deng, X., Gu, L., Liu, C., Lu, T., Lu, F., Lu, Z., et al. Arginine methylation mediated by the Arabidopsis homolog of PRMT5 is essential for proper pre-mRNA splicing. Proceedings of the National Academy of Sciences of the United States of America. 2010, 107, 19114-9.

[7] Andreu-Perez, P., Esteve-Puig, R., de Torre-Minguela, C., Lopez-Fauqued, M., Bech-Serra, J.J., Tenbaum, S., et al. Protein Arginine Methyltransferase 5 Regulates ERK1/2 Signal Transduction Amplitude and Cell Fate Through CRAF. Science Signaling. 2011, 4, ra58-ra.

[8] Nishida, K.M., Okada, T.N., Kawamura, T., Mituyama, T., Kawamura, Y., Inagaki, S., et al. Functional involvement of Tudor and dPRMT5 in the piRNA processing pathway in Drosophila germlines. The EMBO Journal. 2009, 28, 3820-31.

[9] Kanda, M., Shimizu, D., Fujii, T., Tanaka, H., Shibata, M., Iwata, N., et al. Protein arginine methyltransferase 5 is associated with malignant phenotype and peritoneal metastasis in gastric cancer. Int. J. Oncol. 2016, 49, 1195-202.

[10] Zhang, B., Dong, S., Zhu, R., Hu, C., Hou, J., Li, Y., et al. Targeting protein arginine methyltransferase 5 inhibits colorectal cancer growth by decreasing arginine methylation of eIF4E and FGFR3. Oncotarget. 2015, 6, 22799-811.

[11] Tarighat, S., Santhanam, R., Frankhouser, D., Radomska, H.S., Lai, H., Anghelina, M., et al. The dual epigenetic role of PRMT5 in acute myeloid leukemia: gene activation and repression via histone arginine methylation. Leukemia. 2016, 30, 789-99.

[12] Antonysamy, S., Bonday, Z., Campbell, R.M., Doyle, B., Druzina, Z., Gheyi, T., et al. Crystal structure of the human PRMT5:MEP50 complex. Proceedings of the National Academy of Sciences of the United States of America. 2012, 109, 17960-5.

[13] Smil, D., Eram, M.S., Li, F., Kennedy, S., Szewczyk, M.M., Brown, P.J., et al. Discovery of a Dual PRMT5-PRMT7 Inhibitor. ACS medicinal chemistry letters. 2015, 6, 408-12.

[14] Bonday, Z.Q., Cortez, G.S., Grogan, M.J., Antonysamy, S., Weichert, K., Bocchinfuso, W.P., et al. LLY-283, a Potent and Selective Inhibitor of Arginine Methyltransferase 5, PRMT5, with Antitumor Activity. ACS medicinal chemistry letters. 2018, 9, 612-7.

[15] Ye, F., Zhang, W., Ye, X., Jin, J., Lv, Z., Luo, C. Identification of Selective, Cell Active Inhibitors of Protein Arginine Methyltransferase 5 through Structure-Based Virtual Screening and Biological Assays. Journal of chemical information and modeling. 2018, 58, 1066-73.

[16] Gerhart, S.V., Kellner, W.A., Thompson, C., Pappalardi, M.B., Zhang, X.P., Montes de Oca, R., et al. Activation of the p53-MDM4 regulatory axis defines the anti-tumour response to PRMT5 inhibition through its role in regulating cellular splicing. Scientific reports. 2018, 8, 9711.

[17] Ye, Y., Zhang, B., Mao, R., Zhang, C., Wang, Y., Xing, J., et al. Discovery and optimization of selective inhibitors of protein arginine methyltransferase 5 by docking-based virtual screening. Organic & biomolecular chemistry. 2017, 15, 3648-61.
[18] Alinari, L., Mahasenan, K.V., Yan, F., Karkhanis, V., Chung, J.H., Smith, E.M., et al. Selective inhibition of protein arginine methyltransferase 5 blocks initiation and maintenance of B-cell transformation. Blood. 2015, 125, 2530-43.
[19] Cavasotto, C.N., Orry, A.J.W. Ligand docking and structure-based virtual screening in drug discovery. Current Topics in Medicinal Chemistry. 2007, 7, 1006-14.
[20] Lipinski, C.A., Lombardo, F., Dominy, B.W., Feeney, P.J. Experimental and computational approaches to estimate solubility and permeability in drug discovery and development settings. Adv Drug Deliv Rev. 2001, 46, 3-26.
[21] Whitty, A. Growing PAINS in academic drug discovery. Future medicinal chemistry. 2011, 3, 797-801.
[22] Jin, W.Y., Ma, Y., Li, W.Y., Li, H.L., Wang, R.L. Scaffold-based novel SHP2 allosteric inhibitors design using Receptor-Ligand pharmacophore model, virtual screening and molecular dynamics. Computational biology and chemistry. 2018, 73, 179-88.
[23] Shelley, J.C., Cholleti, A., Frye, L.L., Greenwood, J.R., Timlin, M.R., Uchimaya, M. Epik: a software program for pK(a) prediction and protonation state generation for drug-like molecules. Journal of computer-aided molecular design. 2007, 21, 681-91.
[24] Friesner, R.A., Banks, J.L., Murphy, R.B., Halgren, T.A., Klicic, J.J., Mainz, D.T., et al. Glide: a new approach for rapid, accurate docking and scoring. 1. Method and assessment of docking accuracy. Journal of medicinal chemistry. 2004, 47, 1739-49.
[25] Zhang, W.Y., Lu, W.C., Jiang, H., Lv, Z.B., Xie, Y.Q., Lian, F.L., et al. Discovery of alkyl bis(oxy)dibenzimidamide derivatives as novel protein arginine methyltransferase 1 (PRMT1) inhibitors. Chemical biology & drug design. 2017, 90, 1260-70.
[26] Mao, R., Shao, J., Zhu, K., Zhang, Y., Ding, H., Zhang, C., et al. Potent, Selective, and Cell Active Protein Arginine Methyltransferase 5 (PRMT5) Inhibitor Developed by Structure-Based Virtual Screening and Hit Optimization. Journal of medicinal chemistry. 2017, 60, 6289-304.
[27] Salomon-Ferrer, R., Case, D.A., Walker, R.C. An overview of the Amber biomolecular simulation package. Wiley Interdisciplinary Reviews-Computational Molecular Science. 2013, 3, 198-210.
[28] Case, D.A., Cheatham, T.E., 3rd, Darden, T., Gohlke, H., Luo, R., Merz, K.M., Jr., et al. The Amber biomolecular simulation programs. Journal of computational chemistry. 2005, 26, 1668-88.
[29] Wang, J., Wolf, R.M., Caldwell, J.W., Kollman, P.A., Case, D.A. Development and testing of a general amber force field. Journal of computational chemistry. 2004, 25, 1157-74.
[30] Jakalian, A., Jack, D.B., Bayly, C.I. Fast, efficient generation of high-quality atomic charges. AM1-BCC model: II. Parameterization and validation. Journal of computational chemistry. 2002, 23, 1623-41.
[31] Wang, J., Wang, W., Kollman, P.A., Case, D.A. Automatic atom type and bond type perception in molecular mechanical calculations. J Mol Graph Model. 2006, 25, 247-60.
[32] Nayar, D., Agarwal, M., Chakravarty, C. Comparison of Tetrahedral Order, Liquid State Anomalies, and Hydration Behavior of mTIP3P and TIP4P Water Models. Journal of chemical theory and computation. 2011, 7, 3354-67.
[33] Roe, D.R., Cheatham, T.E., 3rd. PTRAJ and CPPTRAJ: Software for Processing and Analysis of Molecular Dynamics Trajectory Data. Journal of chemical theory and computation. 2013, 9, 3084-95.
[34] Humphrey, W., Dalke, A., Schulten, K. VMD: visual molecular dynamics. Journal of molecular

graphics. 1996, 14, 33-8, 27-8.
[35] Miller, B.R., 3rd, McGee, T.D., Jr., Swails, J.M., Homeyer, N., Gohlke, H., Roitberg, A.E. MMPBSA.py: An Efficient Program for End-State Free Energy Calculations. Journal of chemical theory and computation. 2012, 8, 3314-21.
[36] Gohlke, H., Kiel, C., Case, D.A. Insights into protein-protein binding by binding free energy calculation and free energy decomposition for the Ras-Raf and Ras-RalGDS complexes. Journal of molecular biology. 2003, 330, 891-913.
[37] Zhu, K., Jiang, C.S., Hu, J., Liu, X., Yan, X., Tao, H., et al. Interaction assessments of the first S-adenosylmethionine competitive inhibitor and the essential interacting partner methylosome protein 50 with protein arginine methyltransferase 5 by combined computational methods. Biochemical and biophysical research communications. 2018, 495, 721-7.